Finite Element Modeling of Electric Field Distribution in a Defected XLPE Cable Insulation Under Different Magnitudes of Stressing Voltage

S. H. Sulaiman[1], Mohamad N. K. H. Rohani[2], A. Abdulkarim[1], A. S. Abubakar[1], G. S. Shehu[1], U. Musa[1], A. A. Mas'ud[3], N. Rosle[2] and F. Muhammad-Sukki[4]

[1] Department of Electrical Engineering, Ahmadu Bello University, Zaria-Nigeria
[2]Faculty of Electrical Engineering and Technology, University Malaysia Perlis, Malaysia
[3]Department of Electrical Engineering, Jubail Industrial College, Jubail-KSA
[4]School of Computing, Engineering and the Built Environment, Edinburgh Napier University, Edinburgh, Scotland, UK
shsulaiman@abu.edu.ng

Abstract. Air voids in solid dielectrics affect the performance and lifespan of high voltage (HV) equipment. In this research, electric field distribution within a cross-linked polyethylene (XLPE) HV cable is analyzed using a finite element analysis (FEA) software, COMSOL Multiphysics. The study was performed in the presence of air cavity of different sizes within the insulation. The average as well as the maximum field strengths for both 2D and 3D of the healthy cable were observed to be equal under five (5) stressing voltage levels. The local field for 1mm cavity radius in 3D was however lower than that of 2D model with an approximate percentage decrease of 9% for all the applied voltages. Further investigations on the 3D model show that average field rises with voltage and slightly decreases with increasing cavity size, while field enhancement is affected more by the cavity size than voltage stress.

Keywords: Finite element analysis, XLPE, Electric Field, Cable, COMSOL

1 Introduction

In order to provide an uninterruptible power supply to customers, ensuring the reliability of power system networks becomes a necessity. High voltage (HV) installations like power cables and transformers are integral parts of modern power networks, and proper monitoring of their conditions defines the overall efficiency and reliability of the system [1]. Operation of HV equipment relies on quality of insulation [2] which must cope with the varying operating stresses to avoid fast deterioration of the insulation systems and ensure satisfactory operation.

Insulation deterioration and breakdown due to factors like partial discharge (PD) and water treeing are major concerns in HV equipment [1] and [3]. Air voids, protrusions or cracks in or/and on the dielectric serve as PD initiation regions [4]. A sustained PD may lead to total breakdown [5]. PD measurement is therefore employed for diagnostics in HV systems. Accurate modeling and estimation of the field strength and distribution within PD initiating sources aids the understanding of HV installations behavior of [6].

Most researches have utilized simple 2D models to study the impact of electric field in voids of different geometries and sizes [7-9]. Although appreciable results were obtained from these works, the 2D model in the literature is still inadequate as it does not depict a practical cable. In this paper, electric field distribution within an XLPE cable is analyzed in 2D and 3D models considering two scenarios; Case 1: healthy cable and Case 2: with a single spherical void. The field distribution as a function of void radius and applied voltage was investigated, and the two models were compared. Capabilities of COMSOL were utilized in the development and simulation of the model. Further analyses were then carried out on the 3D to examine the relationship between voltage magnitude, cavity size and field strength.

2 Materials and methods

The material properties of the cable model used in this work are adopted from [7] as presented in Table 1, while its geometrical specifications are given in Table 2.
Under applied voltage, U_0, the void is exposed to a local field, E_0, given by [8]:

$$E_0 = -\nabla U_0 \quad (1)$$

Involving the free charge, the electric field displacement is represented as [3]:

$$\nabla . \mathrm{D} = \rho_j \quad (2)$$

where ρ_j is free charge density and $D = \varepsilon_0 E$. The material property, ε, and the charge density, ρ, are related by the Poisson's equation [4]:

$$\nabla^2 U_0 = -\frac{\rho}{\varepsilon} \quad (3)$$

Equation 3 can be solved through finite element approach.

Insulation charge density may be neglected. For voids with extremely small size, void charge density is negligible [4] and [5]. In that case, Equation 3 reduces to [6]:

$$\nabla^2 U_0 = 0 \quad (4)$$

The sinusoidal voltage U_0 is given as [6]:

$$U_0 = U_m sin 2\pi f t \quad (5)$$

where f is the frequency and U_m is the peak value of the applied voltage. The boundary condition between two media is given by [4]:

$$n.(\vec{D}_1 - \vec{D}_2) = \rho_s \quad (6)$$

where, ρ_s is surface charge, while $n.\vec{D}_1$ and $n.\vec{D}_2$ are normal components of electric displacement of any two different mediums.

Table 1. Cable material properties

Material	Conductivity (S/m)	Relative Permittivity
Copper	5.85×10^{7}	1
Aluminum	3.57×10^{7}	2.2
XLPE	1.0×10^{-15}	2.3
Graphite	3.0×10^{-3}	500
PVC	1.0×10^{-15}	2.9
Air	1.0×10^{-100}	1

Table 2. Geometry of the XPLE Cable Model

Layer	Component	Material	Value (mm)
1	Conductor radius	Copper	9.2
2	Inner sheath thickness	Graphite	1.8
3	Insulation thickness	XLPE	7.6
4	Insulation screen	Graphite	2.5
5	Earthing screen thickness	Copper	0.8
6	Bedding	PVC	1.3
7	Armor wire thickness	Aluminum	1.3
8	Outer sheath thickness	PVC	1.3

2.1 Field (Electric and Potential) Equations

Neglecting the surface charges of the insulation material, Equation (6) becomes [4]:

$$n.(\vec{D}_1 - \vec{D}_2) = 0 \tag{7}$$

Equation (8) describes the field enhancement factor, η, [6].

$$\eta = \frac{E_0 - E_1}{E_1} \times 100\% \tag{8}$$

E_0 is the average field at the center of the void, E_1 is the field in a healthy cable at the same coordinate with E_0. The center of the void in this work is at $x = 13.7$ mm, $y = 0.0$ mm for 2D and $x = 13.7$ mm, $y = 0.0$ mm, $z = 25$ mm for 3D model.

2.2 Cable Model

The model geometry in [7] was used for 2D for field strengths evaluation along a cut-line that dissects the insulation through the void diameter and emanates from the cable center at P_1 ($x_1 = 0.0$ mm, $y_1 = 0.0$ mm) to the outer sheath at P_2 ($x_2 = 25.8$ mm, $y_2 = 0.0$ mm). A 3D model with the same properties was developed and meshed as shown in Figs. 1(a) and (b) respectively. The 3D cutline starts at P_1 ($x_1 = 0.0$ mm, $y_1 = 0.0$ mm, $z_1 = 25$ mm) to P_2 ($x_2 = 25.8$ mm, $y_2 = 0.0$ mm, $z_2 = 25$ mm) along work plane shown in Fig. 1(c). The radius of the void is 1.0 mm for both 3D and 2D results.

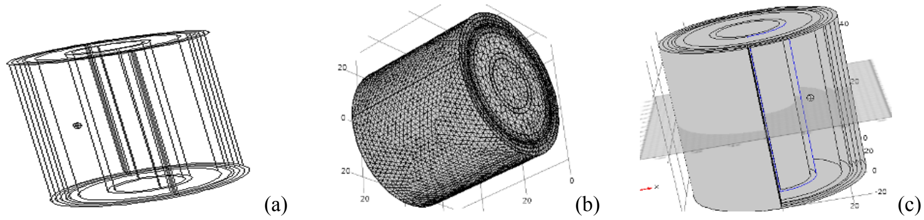

Fig. 1. 3D Cable Model (a) wireframe showing void (b) meshed (c) work plane

3 Results

3.1 Electric Field Distributions in 2D and 3D Models

Field distribution for healthy cable in both 2D and 3D models are shown in Figs. 2 (a) and (b) respectively. The simulation was performed under 18 kV, 50 Hz AC supply using a time dependent study, and the results were recorded at 0.005 s. Maximum field around the HV electrode is 3.12 kV/mm in both cases. The model was then simulated with a void of 1 mm radius, and field behavior was observed. Maximum field in 2D and 3D were 3.65 kV/mm and 3.32 kV/mm respectively as shown in Figs. 2 (c) and (d).

Field distribution along the cutlines is shown in Fig. 3 (a, b and c). Healthy cable in both 2D and 3D is shown in (a), while (b) and (c) show defective cable in 2D and 3D respectively. In the case of defective cable, maximum field occurs inside the void at the point closest to the HV electrode. The whole void has higher field than the insulation.

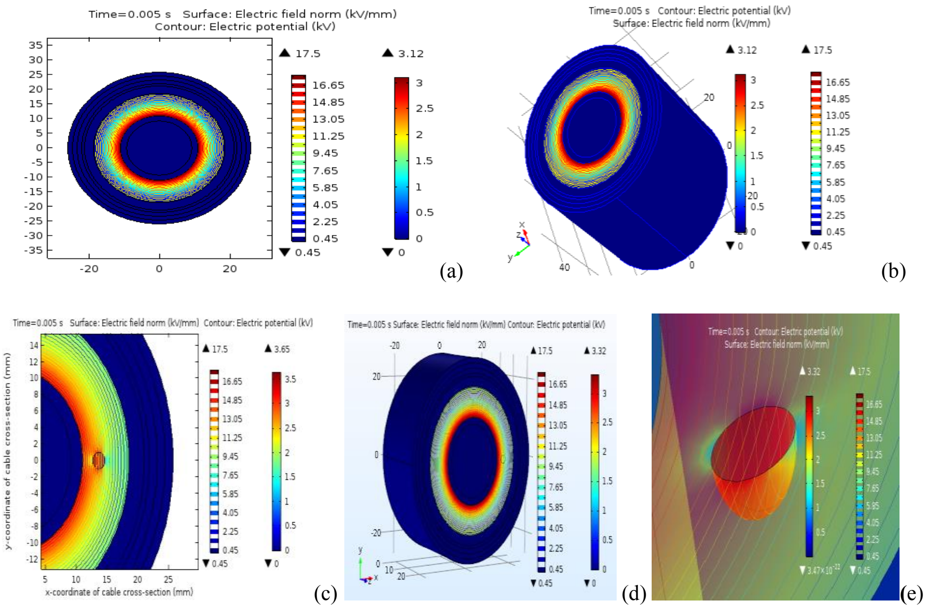

Fig. 2. Electric Field and Potential Distributions (a) 2D healthy (b) healthy 3D Field and (a) 2D defective (b) 3D defective (c) 3D closeup view along work plane

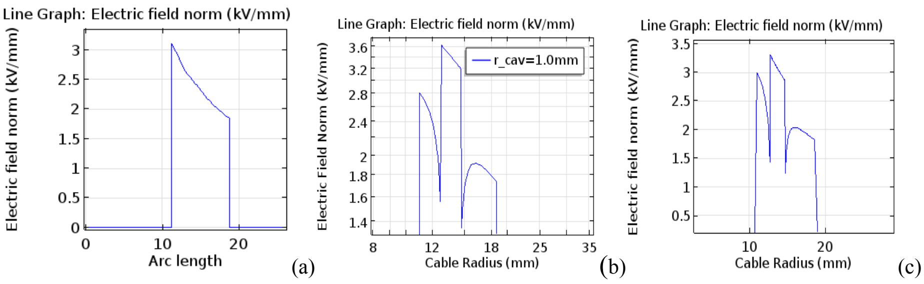

Fig. 3. Field Distribution along cutlines (a) healthy 2D/3D (b) 2D defective (c) 3D defective

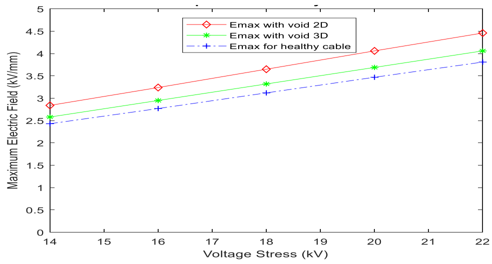

Fig. 4. Maximum Field Comparison between Cable Models

Fig. 4 shows a comparison of the maximum fields in the 2D and 3D as a function of voltage for a 1 mm void radius. In a healthy cable, the two models produced similar results regardless of the voltage. However, for a defective cable, the 2D model has higher field magnitudes than the 3D by around 9% under all voltages.

3.2 Effect of Void Size on Local Field Under Different Voltages

Effect of void size on the local field magnitudes under different values of the stress voltage and fixed void center is examined on the 3D model. Average fields were recorded at the void centers for cavity radii of 0.25, 0.5, 1.0 and 1.5 mm.

Fig. 5 (a) shows variation of average fields with void size at different voltages. In all cases, the field significantly increases with increase in voltage and slightly with decrease in void sizes. In Fig. 5 (b), smaller voids have more impact on field enhancement.

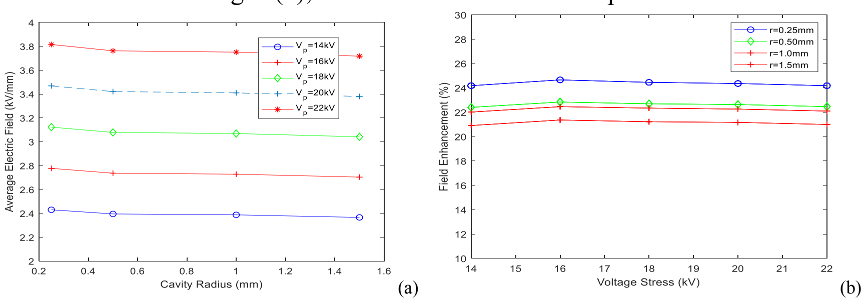

Fig. 5. Impact of void radius and voltage on (a) Average Field (b) Field Enhancement

4 Conclusion

In this paper, 3D and 2D models of an XLPE cable were developed for electric field analysis. This research has established the closeness in field results between 2D and 3D models of healthy cable. However, significant difference was observed when a defect exists within the insulation bulk. For a cavity of 1 mm radius, maximum field strengths in 3D model were always less than those in 2D model by about 9% for all stress voltages considered in this work. Finally, average field was observed to rise with voltage stress but decreases slightly with increase in void sizes, while field enhancement is more affected by cavity size than voltage stress.

Acknowledgement

This work is supported by the Ministry of Higher Education Malaysia under the Fundamental Research Grant Scheme (FRGS/1/2019/TK04/UNIMAP/03/8)

References

1. Negm, T. S., Refaey, M., Hossam-Eldin, A. A.: Modeling and simulation of internal Partial Discharges in solid dielectrics under variable applied frequencies, *18th Int. Middle-East Power Syst. Conf. MEPCON*, pp. 639–644. (2017)
2. Mas'ud, A. A., Musa, U., Sulaiman, S. H., Mahmud, I., Shehu, I. A., Aliyu, B. D.: Partial Discharge Detection and Classification : Implications on the Power Industry, in *18th Int. Conf. and Exhib. on Power and Telecom.s (ICEPT)*, pp. 146–152. (2022)
3. Hore, S., Basak, S., Haque, N., Dalai, S., Mukherjee, M.: Studies on the effect of void geometry and location on electric field distribution and partial discharge in XLPE insulated power cable by finite element analysis using COMSOL multiphysics simulation, *6th Int. Conf. Comput. Appl. Elect. Eng. - Recent Adv. CERA*, pp. 220–225. (2018)
4. Joseph, J.: Classification of PD Sources In XLPE Cables By Artificial Neural Networks And Support Vector Machine, in *IEEE Electr. Insul. Conf. (EIC)*, pp. 407–411. (2018)
5. Musa, U., Mati, A. A., Mas' ud, A. A., Shehu, G. S., Albarracin-Sanchez, R., Rodriguez-Serna, J. M.: Modeling and analysis of electric field variation across insulation system of a MV power cable. In *Int. Conf. on Electr., Comm. & Comp. Eng. (ICECCE)* pp. 1-5. (2021).
6. He, M., Chen, G., Lewin, P. L.: Field distortion by a single cavity in HVDC XLPE cable under steady state, *Inst. Eng. Technol.*, vol. 1, no. 3, pp. 107–114, (2016).
7. Emna, K., Rabah, A., Nejib, C.: Numerical Modeling of the Electric Field and the Potential Distributions in Heterogeneous Cavities inside XLPE Power Cable Insulation, *J. Electr. Electron. Eng.*, vol. 9, no. 2, pp. 37–42 (2016).
8. Musa, U., Mati, A. A., Mas' ud, A. A., Shehu, G. S.: Finite Element Modeling of Fields Distributions in a Three-core XLPE Cable with Multiple Cavities. In 2021 IEEE PES/IAS PowerAfrica (pp. 1-4). IEEE (2021).
9. Alsharif, M., Wallace, P. A., Hepburn, D. M., Zhou, C.: FEM Modeling of Electric Field and Potential Distributions of MV XLPE Cables Containing Void Defect, in *Excerpt from the Proceedings of the COMSOL Conference in Milan,* pp. 1-4 (2012).